Pergamon

Bioorganic & Medicinal Chemistry, Vol. 3, No. 10, pp. 1313–1324, 1995

0968-0896/95 $9.50 + .00

0968-0896(95)00118-2

Identification of an Aldose Reductase Inhibitor Site by Affinity Labeling

Peter F. Kador,[a]* Yong S. Lee,[a] Libaniel Rodriguez,[a] Sanai Sato,[a] Anita Bartoszko-Malik,[a] Yasser S. Abdel-Ghany[b] and Duane D. Miller[b†]

[a]*Laboratory of Ocular Therapeutics, National Eye Institute, National Institutes of Health, Bethesda, MD 20892, U.S.A.*
[b]*Division of Medicinal Chemistry and Natural Products, College of Pharmacy, The Ohio State University, Columbus, OH 20814, U.S.A.*

Abstract—Animal studies indicate that aldose reductase inhibitors represent a pharmacological method for inhibiting the onset of diabetic complications that is independent of blood sugar control. This has spurred the development of aldose reductase inhibitors (ARIs). To facilitate the rational development of more potent and direct ARIs, more specific knowledge of the structural and pharmacophoric requirements of the site at which ARIs interact are required. Co-crystallization of human placental aldose reductase with the inhibitor zopolrestat has been reported to result in a complex where the inhibitor is almost completely sequestered in the hydrophobic pocket which forms the substrate site. Zopolrestat's observed location, which makes the active site pocket inaccessible to solvent or further productive binding of substrate, is not supported by published inhibitor structure–activity relationships (SAR) studies or kinetic results which indicate that aldose reductase inhibitors such as zopolrestat are either non-competitive or uncompetitive inhibitors. Using a 5-iodoacetamido analog of alrestatin as an affinity labeled aldose reductase inhibitor, an inhibitor binding site on aldose reductase has been located. This inhibitor binding site contains a number of pharmacophoric elements previously proposed for the inhibitor site. Its location and composition is consistent with reported kinetic data, SAR observations, stereochemical requirements, and quantum chemical calculations.

Introduction

Recent results from the Diabetes Control and Complications Trials (DCCT) conclude that very tight control of hyperglycemia is beneficial in delaying the onset and progression of retinopathy, neuropathy and nephropathy.[1] This observation corresponds with mounting experimental evidence that links the abnormal accumulation of sorbitol to the development of diabetic complications.[2,3] Sorbitol is a sugar alcohol that is formed by the reduction of glucose by the NADPH-dependent enzyme aldose reductase (AR). Animal studies demonstrate that aldose reductase inhibitors (ARIs), when administered from the onset of hyperglycemia, prevent the onset and progression of polyol accumulation-linked complications in a dose-dependent manner.[2–4] These prevention studies, which indicate that aldose reductase inhibitors represent a pharmacological method for inhibiting the onset of diabetic complications that is independent of blood sugar control, have spurred the development of aldose reductase inhibitors.

While a number of structurally diverse aldose reductase inhibitors have been developed, many possess side effects independent of their ability to inhibit aldose reductase. These include 'hydantoin rash' associated with the presence of the imidazolidine-2',4'-dione group in several inhibitors and the elevation of hepatic transaminases with several non-hydantoin inhibitors.[5] To facilitate the rational development of more potent ARIs devoid of side effects, greater knowledge of the structural and pharmacophoric requirements of the site at which ARIs interact is required. Crystallographic data from human placental aldose reductase indicates that the enzyme differs from other reductases in that it folds into an α/β barrel with a core of eight parallel β strands, the adjacent strands of which are connected by eight peripheral α-helical segments running parallel to the β sheet.[6] NADPH is bound in an unusual extended conformation across the barrel with the nicotinamide ring centered in a large, deeply elliptical hydrophobic pocket which forms the substrate site at the carboxylate terminal end of the β barrel. Adjacent to the accessible side of the nicotinamide ring, where the substrate or product is presumably located, is an unidentified region of electron density.[6] This unknown electron-dense region was subsequently identified as citric acid which was present at a 25 mM concentration in the crystallization media.[7] Subsequent replacement studies also indicate that cacodylate and glucose-6-phosphate bind to this citrate binding site when present in the crystallization buffer. Co-crystallization with the ARI zopolrestat ((3-{[5-(trifluoromethyl)-2-benzothiazolyl]-methyl}-4-oxo-3*H*-phthalazin-1-yl)acetic acid) also resulted in a complex where the carboxylate group of zopolrestat bound to this region where citrate, cacodylate and glucose-6-phosphate bind. Zopolrestat was almost completely sequestered in the large, deeply

†Present address: Department of Medicinal Chemistry, University of Tennessee, Memphis, Tennessee, U.S.A.

elliptical hydrophobic pocket which forms the substrate site.[8] From its carboxylate binding adjacent to the nicotinamide ring, the inhibitor protruded from the center pocket perpendicular to the NADPH ring with an unusually large number of contacts with the substrate site and a high degree of hydrophobic interaction with essentially the entire substrate pocket at the carboxyl-terminal end of the β barrel. Zopolrestat's observed location in the active site pocket makes the active site inaccessible to solvent or further productive binding of substrate. This contradicts kinetic results which indicate that aldose reductase inhibitors such as zopolrestat are either non-competitive or uncompetitive inhibitors[2,9,10] but not competitive inhibitors. Using the affinity label 5-iodoacetamido-1,3-dioxo-1*H*-benz[*de*]isoquinoline-2(3*H*)-acetic acid, an iodoacetamido analog of the ARI alrestatin,[11] an inhibitor binding site on aldose reductase more consistent with reported kinetic data, SAR observations, stereochemical requirements, and quantum chemical calculations, has been located.

Experimental

Chemistry

Melting points were determined using a Thomas-Hoover melting point apparatus and are uncorrected. Compound structures were confirmed by ^{1}H NMR, elemental analyses and/or MS spectra. ^{1}H NMR spectra were obtained with an IBM NR/250 FTNMR (250 MHz) with D_2O or DMSO-d_6 as solvent and internal reference. Mass spectra of the synthetic compounds were obtained with either a Kratos MS25 RFA or Kratos MS-30 mass spectrometer. FAB mass spectra of isolated protein segments were conducted on a Joel SX102 mass spectrometer using glycerol.

*5-Nitro-1,3-dioxo-1*H*-benz[de]isoquinolin-2(3*H*)-acetic acid.* 3-Nitro-1,8-naphthalic anhydride (2.4 g, 9.9 mmol) and glycine (0.85 g, 11.3 mmol) in dry DMF (20 mL) were refluxed for 2 h. The hot reaction mixture was treated with activated charcoal, filtered and poured over crushed ice to form a yellow precipitate which was collected by filtration and dried to yield 2.5 g (84%) of 5-nitro-1,3-dioxo-1*H*-benz[*de*]isoquinolin-2(3*H*)-acetic acid mp 267–270 °C (lit.[12] mp 273–275 °C).

*5-Amino-1,3-dioxo-1*H*-benz[de]isoquinolin-2(3*H*)-acetic acid.* 5-Nitro-1,3-dioxo-1*H*-benz[*de*]isoquinolin-2(3*H*)-acetic acid (2 g, 6.7 mmol) dissolved in 30 mL of DMF was hydrogenated in a Parr bottle 10% Pd/C (0.2 g) at 50 psi for 5 h. The mixture was treated with activated charcoal, filtered and concentrated under vacuum. Addition of water resulted in the formation of a heavy precipitate which was recrystallized from MeOH to yield 1.75 g (97%) of 5-amino-1,3-dioxo-1*H*-benz-[*de*]isoquinolin-2(3*H*)-acetic acid, mp 290 °C (lit.[12] mp 292 °C).

*5-Iodoacetamido-1,3-dioxo-1*H*-benz[de]isoquinolin-2(3*H*)-acetic acid.* Iodoacetic anhydride (35 mg, 0.1 mmol) was added to a suspension of 5-amino-1,3-dioxo-1*H*-benz[*de*]isoquinolin-2(3*H*)-acetic acid (10 mg, 0.037 mmol) in dry THF (5 mL) and refluxed for 1 h. The solvent was evaporated under vacuum and the remaining residue was dissolved in a minimum amount of acetone and precipitated with water to give 15 mg (95%) of 5-iodoacetamido-1,3-dioxo-1*H*-benz[*de*]isoquinolin-2(3*H*)-acetic acid mp 230–234 °C (lit.[11] mp 223–225 °C).

*^{14}C-5-Iodoacetamido-1,3-dioxo-1*H*-benz[de]isoquinolin-2(3*H*)-acetic acid.* ^{14}C-Iodoacetic anhydride (66.63 mg, 0.188 mmol 1.316 mCi, specific activity = 7 mCi mmol^{-1}, prepared from [2-^{14}C]-iodoacetic acid and [2-^{14}C]-iodoacetylchloride by American Radiolabeled Chemicals, Inc.) was added to a suspension of 5-amino-1,3-dioxo-1*H*-benz[*de*]isoquinolin-2(3*H*)-acetic acid (20.18 mg, 0.075 mmol) in dry THF (15 mL). The reaction mixture was refluxed for 3 h and stirred at room temperature overnight. Solvent was evaporated under vacuum and the remaining residue was redissolved in *ca* 5 mL of acetone and then precipitated with water. The precipitate was collected by filtration and dried to give 25.35 mg of ^{14}C-5-iodoacetamido-1,3-dioxo-1*H*-benz[*de*]isoquinolin-2(3*H*)-acetic acid (77% chemical yield; 0.132 mCi, 10% radiochemical yield, specific activity 2.29 mCi mmol^{-1}) mp 230 °C.

Biology

Enzyme assay. Reductase activity was spectrophotometrically assayed on a Shimadzu UV2100U spectrophotometer by following the decrease in the absorption of NADPH at 340 nm over a 4 min period with DL-glyceraldehyde as substrate.[11] Each 1.0-mL cuvette contained equal units of enzyme, 0.10 M Na,K phosphate buffer, pH 6.2, 0.3 mM NADPH with/without 10 mM substrate and inhibitor. Appropriate controls were employed to negate potential changes in the absorption of nucleotide and/or protein modification reagents or aldose reductase inhibitors at 340 nm in the absence of substrate.

Enzyme purification. Recombinant rat lens aldose reductase[13] was purified by a series of chromatographic procedures as previously described.[13] Briefly, aldose reductase was released from *Escherichia coli* by sonication and the mixture was centrifuged at 10,000 × *g* for 10 min. The obtained supernatant was applied to a Sephadex G-75 column (2.5 × 90 cm) equilibrated with 10 mM imidazole–HCl buffer, pH 7.5 containing 7 mM 2-mercaptoethanol and eluted with the same imidazole buffer. The eluent was collected in 220-drop aliquots (*ca* 10 mL) and fractions containing aldose reductase activity were applied to a Matrex Gel Orange A column (2.5 × 15 cm). The column was washed with the imidazole buffer (*ca* 500 mL) and the enzyme was then eluted with the same imidazole buffer containing 0.1 mM NADPH. Fractions eluted with NADPH were chromatofocused on a Mono P (HR 5/20) column developed at a flow rate of 1 mL min^{-1} with Polybuffer 74 (diluted 10-fold and containing 7 mM 2-mer-

captoethanol). The protein concentration of the eluent was monitored at 280 nm and peaks containing aldose reductase activity were collected and concentrated on Centricon 10 filters to a concentration of *ca* 1 mg mL^{-1}.

Affinity binding. Rat lens aldose reductase was passed through a NAP-5 desalting column (Pharmacia LKB, Piscataway, NJ) equilibrated with 0.1 M sodium phosphate buffer, pH 7.6 to remove 2-mercaptoethanol. After determining the concentration of the dialyzed protein by the method of Bradford,[15] an equal millimolar amount of 5-iodoacetamido-1,3-dioxo-1*H*-benz[*de*]isoquinolin-2(3*H*)-acetic acid dissolved in 0.1 mM sodium phosphate buffer, pH 7.6 was added and the reaction was allowed to proceed at room temperature for 15 min. Unreacted reagent was then removed from the protein by gel filtration through a NAP-5 desalting column with 0.1 M phosphate buffer, pH 7.0, containing 10 mM 2-mercaptoethanol. The protein fraction was concentrated, mixed with 100 mM Tris–HCl buffer, pH 8.5 containing 0.1% SDS and 5% β-mercaptoethanol, and heat denatured in a boiling water bath for 2 min. Sequencing grade trypsin (bovine pancreas, Boehringer Mannheim Biochemica) was then added to the solution in a ratio of 5:100 (w/w) and the protein was digested overnight at 37 °C. Overnight digestion was monitored by SDS-PAGE on a Pharmacia PhastSystem in which proteins were visualized with silver stain. The digested mixture was lyophilized, redissolved in 6 M guanidine hydrochloride, and sep-arated by reversed-phase high pressure liquid chroma-tography on a Vydac C_8 column using a 0–75% linear gradient of A: H_2O–0.18% TFA and B: 40% aqueous acetonitrile–0.18% TFA with a flow rate of 0.5 mL min^{-1}. (LKB HPLC system with model 2150 Pumps, 2152 Controller, and 2151 variable wavelength detector set at 210 nm.) Collected fractions were subjected to FAB mass spectroscopy in the presence of glycerol.

Autoradiography. Sodium dodecyl sulfate-polyacrylamide gel electrophoresis (SDS-PAGE) was performed according to the method of Laemmli[16] using 1.5 mm 15% polyacrylamide gels and bovine serum albumin (67 K), ovalbumin (43 K), carbonic anhydrase (30 K), soybean trypsin inhibitor (20.1 K) and α-lactalbumin (14.4 K) as molecular weight standards. Protein was stained with Coomassie blue stain. After drying on a Pharmacia GSD-4 slab gel dryer, the gel was autoradiographed for 14 days at –60 °C using HYPERFILM-MP (Amersham Life Sciences).

Computer modeling studies

Crystal coordinates of recombinant human aldose reductase complexed with NADPH (AR·NADPH)[6] were obtained from the Brookhaven Protein Data Bank. Using Quanta 3.3/CHARMm22 (Molecular Simulations Inc.), all water molecules were first removed from the crystal structure of AR·NADPH and then polar hydrogen atoms were added to the enzyme. The NADPH cofactor was modified to include all hydrogen atoms with a net charge of –4. The AR·NADPH complex was assumed to carry a net charge of –6 (–2 for AR and –4 for NADPH). Inhibitors were assumed to have a net charge of –1. Charge templates of Quanta 3.3/CHARMm were utilized for assigning partial charges to NADPH and inhibitors.

The geometry of the AR·NADPH complex was optimized on HP-735 and SGI Crimson using the CHARMM[17] program with the Molecular Simulations parameter set.[18] The adopted basis Newton–Raphson algorithm with an energy gradient < 0.01 kcal mol^{-1} $Å^{-1}$ and zero energy tolerance was utilized for geometry optimization. A distance dependent dielectric $D(\varepsilon) = 4r$ was used to approximate electrostatic screening by water molecules. In the absence of water molecules this is a widely used approximation. A cut off at 14.0 Å was used for non-bonded interactions. Non-bonding lists were updated heuristically. Electrostatic interactions were treated with the force switch method[19] and a switching range of 8–12 Å. Van der Waals interactions were calculated with the shift method[19] and a cutoff of 12 Å. No constraints were imposed on geometry optimizations.

Inhibitors were manually docked into the identified inhibitor binding region of the AR·NADPH complex. Interaction energies (ΔE) between the AR·NADPH complex and inhibitors were calculated using the equation $\Delta E = E_{AR\cdot NADPH\cdot I} - [\, E_{AR\cdot NADPH} + E_I \,]$ where $E_{AR\cdot NADPH\cdot I}$, $E_{AR\cdot NADPH}$ and E_I are the energies of the optimized AR·NADPH·inhibitor complex, AR·NADPH complex and inhibitor, respectively.

Results

Based on previous studies which indicate that the 5-iodoacetamido-affinity-labeled analog of the ARI alrestatin (5-iodoacetamido-1,3-dioxo-1*H*-benz[*de*]isoquinoline-2(3*H*)-acetic acid) selectively binds rat lens aldose reductase,[11] radiolabeled 5-iodoacetamido-1,3-dioxo-1*H*-benz[*de*]isoquinoline-2(3*H*)-acetic acid possessing ^{14}C in the α-acetyl position of the iodoacetamido group was prepared by reacting ^{14}C-iodoacetic anhydride with 5-amino-1,3-dioxo-1*H*-benz[*de*]isoquinolin-2(3*H*)-acetic acid. Equimolar amounts of this inhibitor dissolved in 0.1 M Na,K phosphate buffer, pH 7.4, were combined with recombinant rat lens aldose reductase[13] purified through a series of chromatographic steps which included gel filtration on Sephadex G-75, affinity chromatography on Matrex Gel Orange A, chromatofocusing on a Mono P column, and then dialyzed against 0.1 M Na,K phosphate buffer pH 7.4.[14] Following removal of unreacted affinity label by gel filtration, the affinity labeled enzyme was heat denatured and digested overnight with trypsin. Autoradiography of the SDS-PAGE of an aliquot of the digested protein indicated that alkylation of radiolabel was limited and apparently specific (Fig. 1). The digested mixture was then lyophilized, redissolved in 6 M guanidine hydrochloride, and separated by reversed-phase HPLC on a Vydac C_8 column (Fig. 2). The location of the inhibitor-bound fractions was identified

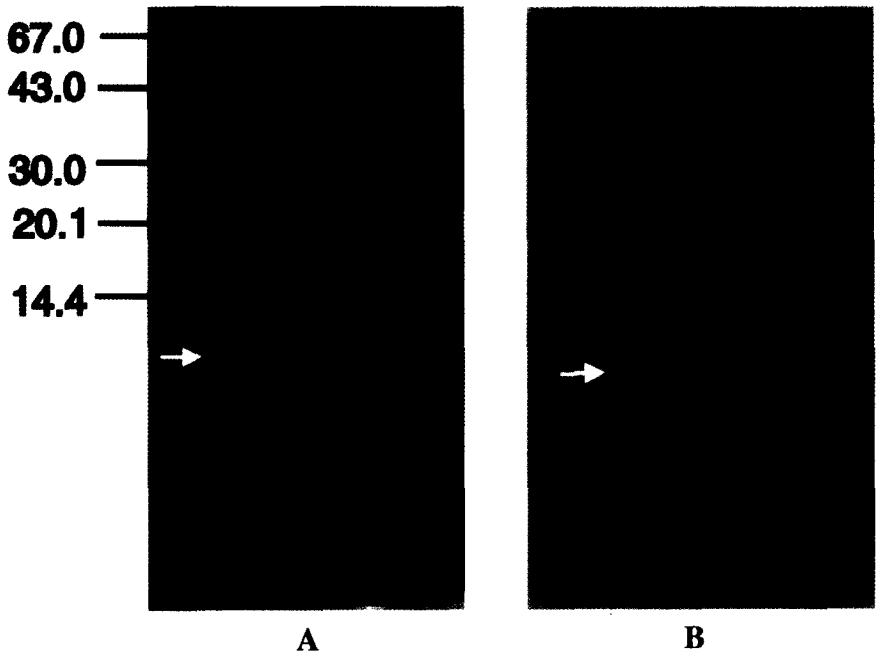

Figure 1. SDS-PAGE stained with Coomasie Blue (**A**) and autoradiograph (**B**) of trypsin-digested rat lens aldose reductase reacted with radiolabel 5-iodoacetamido-alrestatin. Identical digest was applied to two lanes in **A** while the third lane contained the molecular weight standards bovine serum albumin (67 K), ovalbumin (43 K), carbonic anhydrase (30 K), soybean trypsin inhibitor (20.1 K) and α-lactalbumin (14.4 K). The black arrows in **A** indicate molecular weights while the white arrows in **A** and **B** indicate the corresponding location of protein fragments containing radiolabel. The gel was slightly overloaded to demonstrate the limited nature and apparent specificity of the label. Please note that the author has enhanced the gel in order to sharpen the bands.

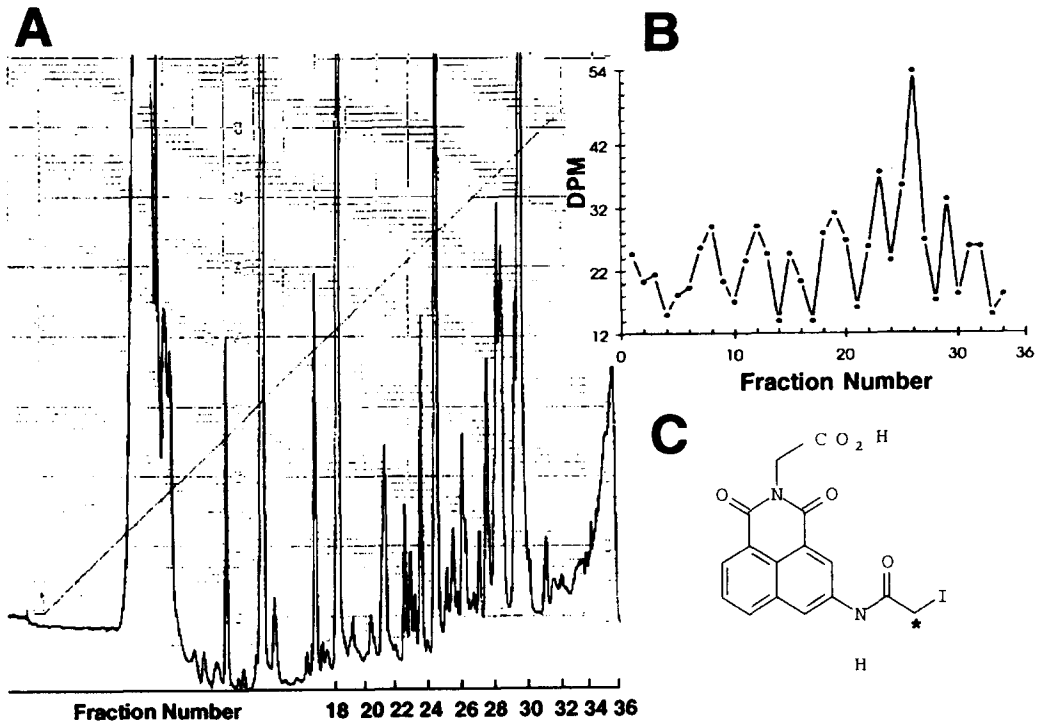

Figure 2. Separation and identification of protein fractions containing radiolabel from trypsin-digested rat lens aldose reductase labeled with radiolabel 5-iodoacetamido-alrestatin. **A** illustrates protein separations detected at 210 nm obtained by reversed-phase HPLC on a Vydac C_8 column using a 0–75% linear gradient of A: H_2O–0.18% TFA and B: 40% aqueous acetonitrile–0.18% TFA with a flow rate of 0.5 mL min^{-1}. The location of fractions containing radiolabel was subsequently determined through liquid scintillation counting (**B**). **C** illustrates the chemical structure of ^{14}C-5-iodoacetamido-1,3-dioxo-1*H*-benz[*de*]isoquinolin-2(3*H*)-acetic acid.

by analyzing each fraction collected on a liquid scintillation counter. The entire procedure was then repeated with non-radiolabeled 5-iodoacetamido-1,3-dioxo-1*H*-benz[*de*]isoquinoline-2(3*H*)-acetic acid and isolated fractions corresponding to previously identified inhibitor-bound fractions were analyzed by mass

spectrometry. Using FAB-MS and collision MS a mixture of two inhibitor-bound fragments were observed which corresponded to the tryptic fragments ^{264}Ser-Val-Thr-Pro-Ala-Arg^{269} and ^{34}Val-Ala-Ileu-Asp-Met-Gly-Tyr-Arg^{41}. Identification of ^{264}Ser-Val-Thr-Pro-Ala-Arg^{269} was based on the appear-ance of a 940 mass peak and a 629 mass peak where the inhibitor fragment (311) was removed. The second fragment ^{34}Val-Ala-Ileu-Asp-Met-Gly-Tyr-Arg^{41} was identified by the presence of peaks at masses 1235, 1251 (methionine sulfoxide), 1267 (methionine sulfone), 924 (-inhibitor fragment) and 941 (sulfoxide-inhibitor fragment). Based on the chemical nature of the affinity label, the label was deduced to be bound to ^{263}Ser and ^{40}Tyr of rat lens aldose reductase. Because of the close homology between the rat lens and human placental aldose reductase,[20,21] these residues correspond to ^{263}Ser (^{263}Ser-Val-Thr-Pro-Glu-Arg^{268}) and ^{39}Tyr (^{33}Val-Ala-Ileu-Asp-Val-Gly-Tyr-Arg^{40}). In addition to similar primary structures, comparison of rat lens to human placental aldose reductase is justified because both enzymes have similar kinetic properties, activation by sulfate, inhibition by chloride, and relative inhibition profiles with aldose reductase inhibitors.[20]

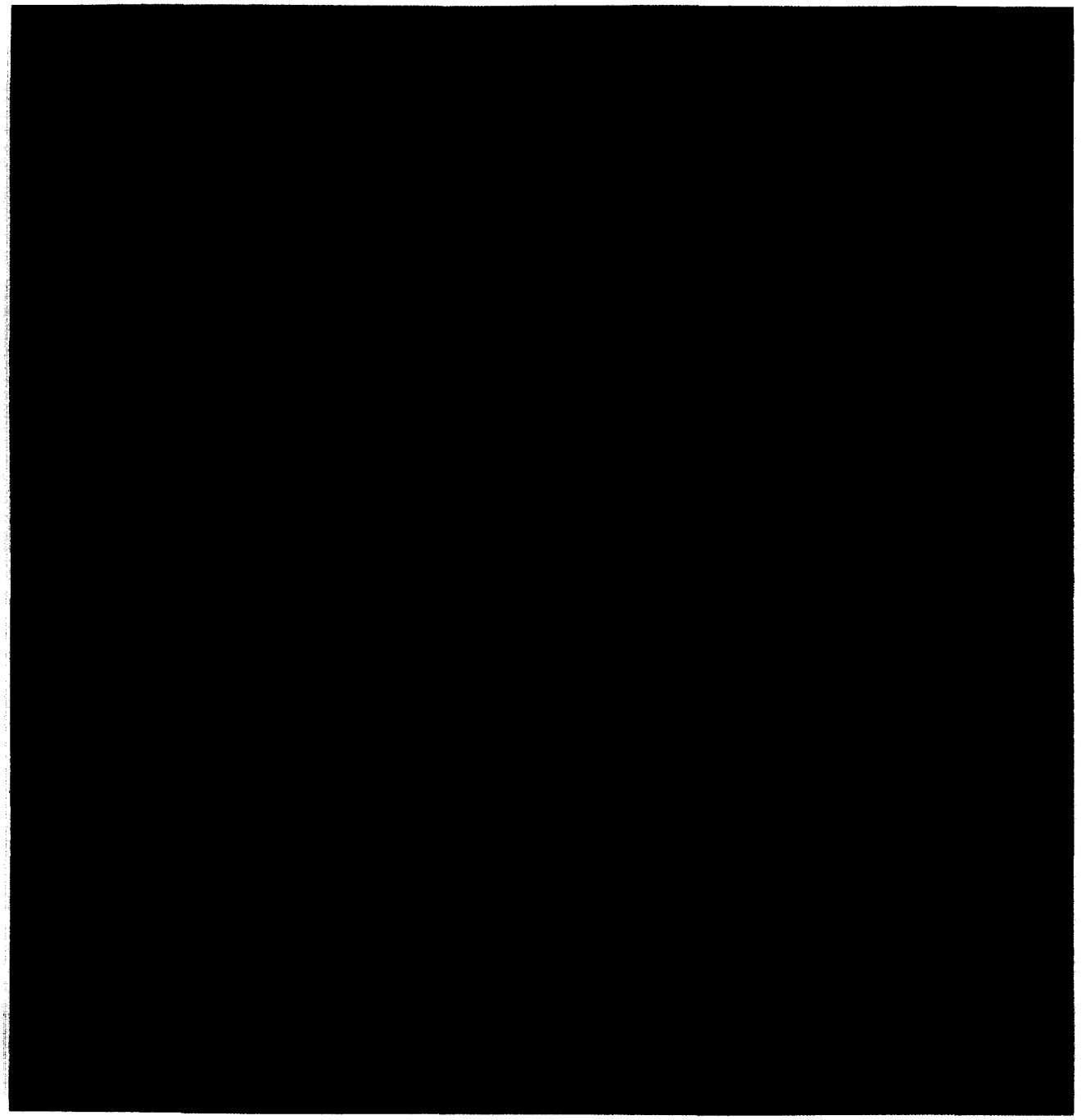

Figure 3. Optimized structure of aldose reductase illustrating the location of the identified inhibitor site (yellow box) in which ^{39}Tyr and ^{263}Ser are located in close proximity to the adenine ring of the nucleotide cofactor and the substrate site (red box).

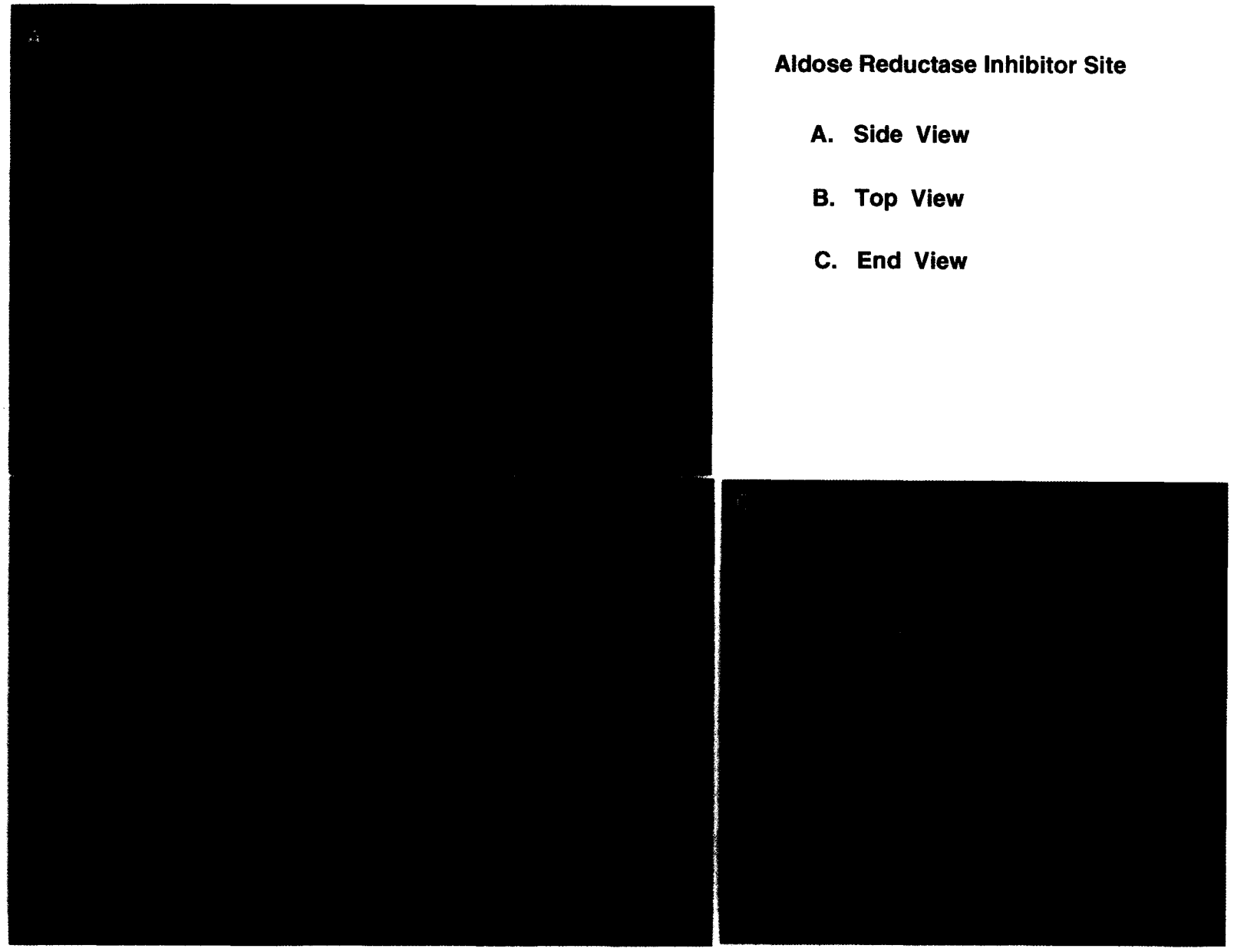

Figure 4. Side, top and end view of the identified inhibitor site of aldose reductase illustrating the location of the nucleophilic ^{39}Tyr and ^{263}Ser residues, the carboxylate binding ^{268}Arg, adenine ring of the bound NADPH which forms the primary lipophilic (van der Waals' interactive) binding region and ^{261}Pro which represents the secondary lipophilic (van der Waals' interactive) binding region Distances are summarized in Table 1.

The two identified residues were localized on the optimized structure of recombinant human aldose reductase complexed with NADPH (AR·NADPH) derived from crystal coordinates[6] using Quanta 3.3/CHARMm22 after all water molecules were removed from the crystal structure and polar hydrogen atoms were added. In the optimized structure of the AR·NADPH complex, ^{39}Tyr and ^{263}Ser are located in close proximity to the adenine ring of the nucleotide cofactor (Fig. 3). Together with the imido group of ^{268}Arg the hydroxyl groups of ^{39}Tyr and ^{263}Ser form a plane that is nearly parallel to a plane formed by the adenine ring and ^{261}Pro. As illustrated in Figure 4, between the two planes is a deep, sterically constrained cleft which contains a number of attributes previously proposed for the aldose reductase inhibitor site.[22-24] These include the presence of multiple nucleophilic regions, represented by ^{39}Tyr and ^{263}Ser, a sterically constrained nucleophile containing region (^{39}Tyr), a primary planar lipophilic (van der Waals' interactive) region (adenine ring) and a nearly coplanar secondary lipophilic (van der Waals' interactive) region (^{261}Pro), anionic or carboxylate binding region(s) (^{268}Arg and 6-amino group of adenine ring) and selective hydrogen bonding regions (^{272}Asn, adenine ring). The relative distances between these residues are summarized in Table 1.

To determine whether the identified cleft can theoretically bind other ARIs, a number of structurally diverse inhibitors (Fig. 5) were manually docked into this cleft and the geometry of each docked complex was minimized. Each of the optimized docked complexes was further reoptimized until energy changes of less than 0.05 kcal mol^{-1} were obtained. Manual docking was conducted on the assumption that hydrophobic bonding through van der Walls' interactions occur and that charge-transfer interactions occur through either reversible nucleophilic interaction and/or ionic bonding.[22-26] The negative charges associated with either the carboxylate or hydantoin rings were 'anchored' to this site through either the imine group of ^{268}Arg or the 6-amino group of adenine while the adenine ring and ^{261}Pro were used for hydrophobic binding. Interaction energies (ΔE) between the AR·NADPH complex and each inhibitor, calculated using the equation $\Delta E = E_{AR\cdot NADPH\cdot I} - [\, E_{AR\cdot NADPH} + E_I \,]$ where $E_{AR\cdot NADPH\cdot I}$, $E_{AR\cdot NADPH}$ and E_I are the energies of the optimized AR·NADPH·inhibitor complex, AR·NADPH complex and inhibitor, respectively, resulted in energetically favorable interaction between inhibitor and the AR·NADPH site (Table 2). Depending on the alignment of the negative charge of the inhibitors with either ^{268}Arg or the 6-amino group of adenine, several possible conformations of the AR·NADPH·I complex can be formed with the inhibitors. Formation of the AR·NADPH·I complex also resulted in hydrogen bond formations which further 'anchor' the inhibitors to the AR·NADPH complex and acceptable alignments of either ^{39}Tyr and ^{263}Ser for nucleophilic interaction with appropriate inhibitor functional groups. These calculations, however, reflect only intermolecular interactions associated with the 'fit' of the AR·NADPH·I complex and cannot reflect potential nucleophilic interactions between the acceptor and ^{39}Tyr and ^{263}Ser.

Discussion

Crystallographic analyses are an invaluable tool in identifying protein structures and their site of interaction with other molecules. Crystallization of aldose reductase has provided insight into the unusual extended conformation of the NADPH binding conformation of the Enzyme·NADPH complex and the location of the substrate site within a deeply hydrophobic pocket. Subsequent studies have indicated that a number of charged compounds from the buffer medium co-crystallize in the citrate binding site adjacent to the nicotinamide ring within this hydrophobic pocket including citrate, cacodylate, and glucose-6-phosphate. Binding to the same site was also observed in the co-crystallization with zopolrestat where citric acid (from the crystallization buffer) was displaced by the carboxylate group of zopolrestat.[7,8] This location which predicts aldose reductase inhibitors to be competitive rather than uncompetititive or non-competitive inhibitors and assumes that ARIs inhibit merely through anionic bonding, is inconsistent with observed kinetics, SAR and quantum chemical calculations (Table 3).[8,27]

Affinity and photoaffinity labels provide an alternative method for binding site identification. The use of affinity and photoaffinity analogs of known aldose reductase inhibitors as specific probes to gain insight into the nature of aldose reductase inhibition and to refine the initial spatial requirements of the inhibitor site has previously been reported.[11,28-30] Although bind-

Table 1. Residues forming the aldose reductase inhibitor binding site

	Distance in Å					
	Ser O–H	Tyr O–H	Arg =N–H	Adenine –NH_2	Adenine Center*	Pro Center
^{263}Ser O–H	–	7.40	6.46	6.42	5.88	8.24
^{39}Tyr O–H	7.40	–	12.69	8.23	9.61	5.52
^{268}Arg=N–H	6.46	12.69	–	6.63	4.29	11.53
^{261}Pro Center†	8.24	5.52	11.53	8.01	8.14	–
^{272}Asn NH_2	4.55	4.76	8.19	4.29	4.92	4.60

*Center of purine ring.
†Center of pyrrolidine ring.

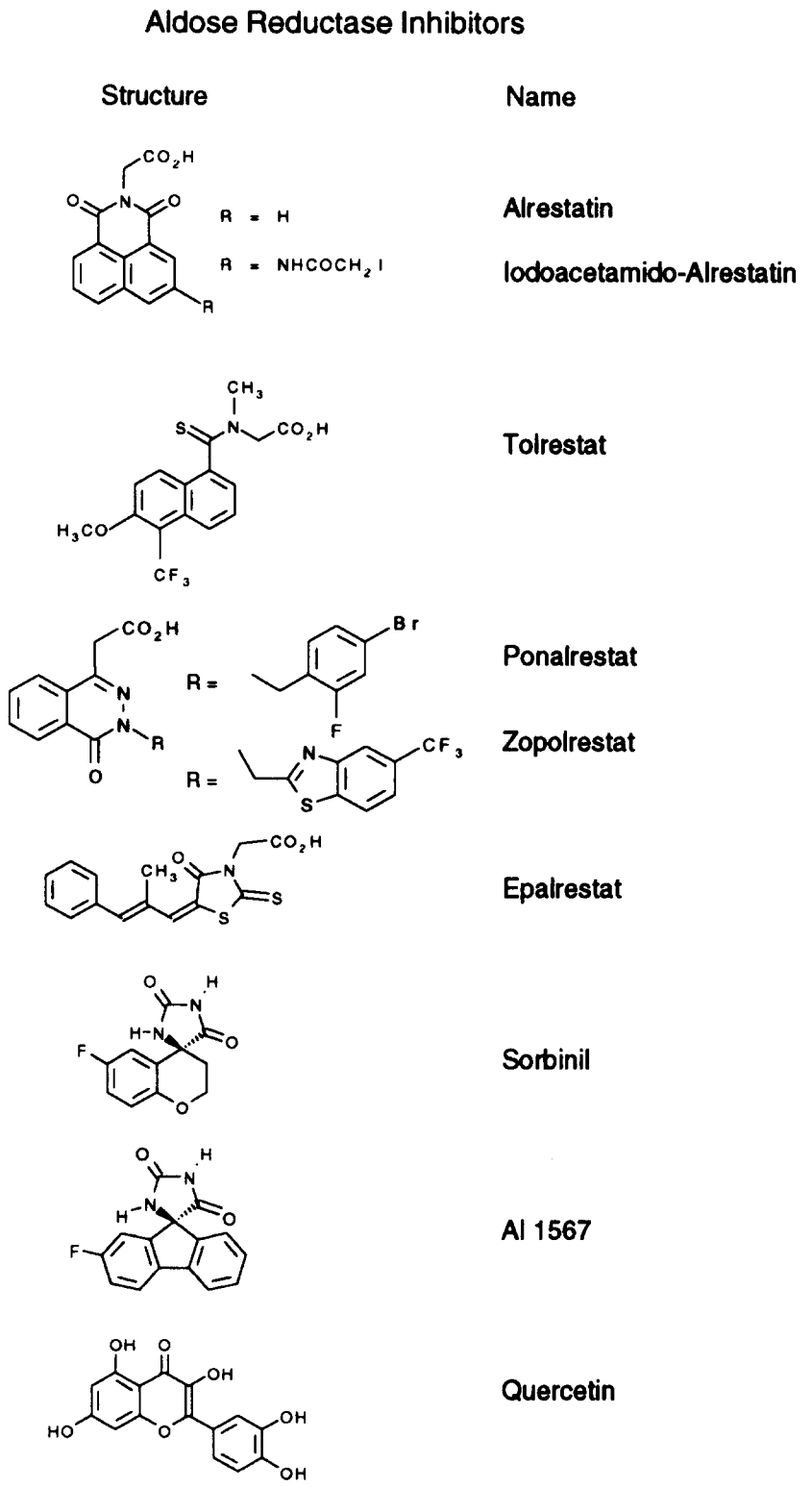

Figure 5. Structures of aldose reductase inhibitors investigated.

ing of these affinity labeled un- or non-competitive inhibitors is less than that observed for classical affinity labeled competitive inhibitors, the selectivity of affinity labeled ARIs has been established through protection and competition studies[11,28-30] and, presently, through autoradiographic analyses. Studies with 5-iodoacetamido-1,3-dioxo-1*H*-benz[*de*]isoquinoline-2(3*H*)-acetic acid, an affinity labeled analog of the ARI alrestatin suggests that inhibitor binding to a sterically constrained cleft located between the imido group of ^{268}Arg, the hydroxyl groups of ^{39}Tyr and ^{263}Ser, and the adenine ring of the nucleotide cofactor is also possible.

Table 2. Summary of inhibitor site binding by aldose reductase inhibitors

Inhibitor		Interaction Energy ΔE (kcal mol^{-1})	Distance (Å) O of ^{39}Tyr to Acceptor*	Distance (Å) O of ^{263}Ser to Acceptor*	Hydrogen Bonding†
Alrestatin[a]	(a)	–21.1	>7	6.56	acid–Arg
	(b)	–17.5	>7	6.53	acid–adenine NH_2
Iodoacetamido Alrestatin[b]	(a)	–27.1	3.67	4.65	acid–adenine NH_2
	(b)	–27.7	6.31	4.14	acid–Arg
	(c)	–23.4	3.61	4.71	amido carbonyl–Asn
Tolrestat[c]	(a)	–7.9	3.27	4.81	
	(b)	–9.9	>7	>7	ϕ-0-CH_3–Ser
Ponalrestat[d]	(a)	–10.6	4.46	6.01	acid–Arg
	(b)	–19.8	>7	3.93	acid–Adenine NH_2
Zopolrestat[e]	(a)	–19.5	>7	>7	4'-cabonyl–Arg N-benzthiazoline–Ans
	(b)	–23.3	>7	>7	acid–Asn 4'-carbonyl–Arg N-benzthiazoline–Ans
	(c)	–25.9	>7	>7	acid–Arg 4'-carbonyl–Asn
Epalrestat[f]	(a)	–15.1	5.21	3.60	acid–Tyr carbonyl–Asn
	(b)	–21.2	>7	5.08	acid–Arg
Sorbinil[g]	(a)	–16.2	6.94	5.88	2'-carbonyl–Asn 1'-imide–Arg
	(b)	–18.9	6.91	3.30	2'-carbonyl–Asn 1-ether O–Arg 1'-imide–adenine
	(c)	–17.9	>7	5.88	2'-carbonyl–Asn 1-ether O–Arg
Al 1567[h]	(a)	–19.8	>7	4.69	4'-carbonyl–Arg 1'-HN–adenine
	(b)	–9.9	>7	5.23	2'–carbonyl–Ser
	(c)	–17.5	>7	4.44	2'-carbonyl–Ser 4'-carbonyl–Arg
Quercetin[i]	(a)	–14.5	5.95	5.40	4-carbonyl–Asn hydroxyls–Arg, Pro, Tyr, Phosphate
	(b)	–30.4	5.56	5.24	4-carbonyl–Asn hydroxyls–Tyr, Pro

a–c represent different conformations.
*Nucleophiles are: [a]1-carbonyl of 1,3-dioxo-1*H*-benz[*de*]isoquinoline-2(3*H*)-acetic acid; [b]α-acetamido position of leaving group of 5-iodoacetamido-1,3-dioxo-1*H*-benz[*de*]isoquinoline-2(3*H*)-acetic acid; [c]thioxcarbonyl of N-[(5-trifluoromethyl-6-methoxy-1-naphthalenyl)thioxomethyl]-N-methylglycine; [d]4-carbonyl of (3-[4-bromo-2-fluorobenzyl]-4-oxo-3*H*-phthalazin-1-yl)acetic acid; [e]4-carbonyl of (3-{[5-(trifluoromethyl)-2-benzothiazolyl]methyl}-4-oxo-3*H* phthalazin-1-yl)acetic acid; [f]1-carbonyl of 5,(*E*)-5-[(*E*)-2'-methyl-3'-phenylpropenylidene]-rhodanine-3-acetic acid; [g]4'-carbonyl of *S*-6-fluorospiro chroman-4,5'-imidazolidine-2',4'-dione; [h]4'-carbonyl of 2-fluorospirofluorene-9,5'-imidazolidine-2',4'-dione; [i]4-carbonyl of 2-(3,4-dihydroxyphenyl)-3,5,7-trihydroxy-4-oxo-4*H*-chromen.
†2.01–2.55 Å.

Binding to this alternate region is more consistent with reported kinetic data, SAR observations, stereochemical requirements, and quantum chemical calculations as summarized in Table 3.

Kinetic studies conducted with reversible, structurally diverse ARIs indicate that aldose reductase is inhibited by either a non-competitive or uncompetitive mechanism when either aldehyde or NADPH is varied. In addition, kinetic and competition studies suggest the ARIs are bound to a single allosteric regulatory site on the enzyme.[26,30–33] Aldose reductase follows a compulsory ordered kinetic mechanism where reduced coenzyme binds before the aldehyde. The AR·NADPH·aldehyde complex is then converted to AR·$NADP^+$·alcohol through a hydride shift which presumably results in a conformational change which allows the release of alcohol and then, the subsequent release of $NADP^+$.[34,35] On the other hand, ARIs are competitive with alcohol substrate in the reverse reaction where the alcohol is oxidized by a hydride shift from the AR·$NADP^+$·alcohol complex to form the AR·NADPH·aldehyde complex.[36,37] Inhibitor binding to the AR·NADPH complex (or AR·NADPH·aldehyde complex) is consistent with these kinetic observations of uncompetitive or non-competitive inhibition since

Table 3. Comparison of inhibitor site characteristics with experimental observations

Experimental Observations	Crystal Structure Identified Site	Affinity Labeled Site
Kinetics indicate un- or non-competitive inhibition with respect to substrate in the forward (reductive) step and competitive in the reverse (oxidative) step[2,3,7,8,10,24,38,39]	Location of substrate site suggests competitive inhibition in both the forward and reverse reaction	Observed allosteric location which may affect release of nucleotide could be un- or non-competitive in forward and competitive in reverse reaction
Both carboxylic acid and non-carboxylic acid containing inhibitors bind to the same site[24,30]	Carboxylate required	Docking studies indicate both carboxylate and non-carboxylate containing ARIs can bind
Hydrophobic substituents enhance inhibitory potency[2,10,12,22,39]	Hydrophobic substituents enhance binding affinity of inhibitors at the substrate site	Site contains adenine ring and nearly coplanar ^{261}Pro for van der Waals interactions
Reactive nucleophile present at site where ARIs interact with protein[11,22,24,29]	No reactive nucleophile available	^{39}Tyr and ^{263}Ser present
Both ionic and nucleophilic charge-transfer interactions can occur[2,23]	Only ionic interaction occurs	Both ionic and nucleophilic charge-transfer interactions can occur
Location of nucleophile is specific[22,23,24,29]	n/a	Yes
Reversible and irreversible ARIs interact at the same site[29,30,41]	No	Yes
Irreversible inhibitors not competitive with substrate or NADPH[24]	n/a	Irreversibly-bound inhibitor is not competitive with substrate or NADPH
Reactive carbonyl groups in non-carboxylic acid containing inhibitors increase inhibitory activity[24]	No	Molecular modeling suggests that nucleophilic interactions with reactive carbonyls possibly occur
4-Nitrobenzenesulfonyl-fluoride suggests tyrosine to be present where ARIs interact with enzyme[24]	No	^{39}Tyr located at site
2-Bromo-4-nitroacetophenone reactivity suggests the presence of a guanidine group in the interaction of ARIs with the enzyme[22]	No	^{268}Arg located at site
Stereoselective inhibition occurs[2,22,31,38]	No	Positions of nucleophiles allows stereospecific inhibition to occur
Inhibitory susceptibility of the stored enzyme is altered depending on inhibitor structure. Marked changes in secondary structure and kinetic properties occur that result in enzyme activation with decreased sensitivity to inhibition by ARIs[24,34]	Relationship of increased substrate activity to decreased inhibition not apparent since more lipophilic inhibitors appear to have greater decrease in ability to inhibit	Altered secondary structure with some unfolding of lipophilic (van der Waals' interactive) regions at the inhibitor site while the adjacent hydrogen bonding regions are less affected could account for differences in reduced inhibitory activity for inhibitors such as sorbinil while quercetin or tolrestat were less affected.

the presence of inhibitor may not interfere with aldehyde binding but could prevent potential allosteric changes required for the release of alcohol from the inhibitor·AR·NADP$^+$·alcohol complex. In the reverse reaction where alcohol is oxidized, the formation of an inhibitor·AR·NADP$^+$ complex could interfere with potential allosteric changes required for the association of alcohol to the AR·NADP$^+$ complex to form the AR·NADP$^+$·alcohol complex. The resulting inhibition would appear competitive with respect to the alcohol substrate.

Previous studies have defined the key features of the AR inhibitor binding region to include a parallel primary and secondary lipophilic (van der Waals' interactive) region, a sterically constrained charge-

transfer pocket where nucleophilic interaction can occur from several possible directions, an anionic binding region and hydrogen bonding groups located adjacent to the lipophilic regions which can help anchor inhibitors to the site.[25-28] These key features are aligned so that stereospecific inhibition can occur.[32,38] The key feature of the present model is that the inhibitor binding region is formed *in situ* after nucleotide binding to the enzyme occurs. The adenine ring forms the primary van der Waals' interactive binding region while ^{261}Pro provides a nearly coplanar secondary van der Waals' interactive binding region. Inhibitor binding to the presently defined AR·NADPH complex is consistent with a previously proposed model for the AR inhibitory site which was based on a combination of AR enzyme inactivation experiments, SAR observations, stereochemical requirements and quantum chemical calculations. Previous kinetic inhibition and inactivation studies of AR 4-nitrobenzenesulfonyl fluoride, a reagent known to inactivate tyrosine residues, and 2-bromo-4'-nitroacetophenone, a reagent which reacts well with guanidine groups, have suggested the presence of both tyrosine and arginine at the enzyme site occupied by inhibitor molecules.[22-26] Molecular modeling studies and quantum chemical calculations have also suggested that charge-transfer interactions can occur in a sterically constrained inhibitor site pocket on the enzyme through nucleophilic interaction with residues at two potential locations and that binding of an acidic inhibitor moiety can occur.[22-25,39] Alignment of the acidic inhibitor moiety with either ^{268}Arg or the 6-amino group of adenine in the proposed AR·NADPH·I complex results in the appropriate positioning of select inhibitor functional groups for nucleophilic interaction with either ^{39}Tyr or ^{263}Ser. This positioning introduces stereochemical constraints which are in agreement with observed stereochemical ARI requirements.

Experimentally, purified aldose reductase often looses its ability to be inhibited by select ARIs. This loss of inhibition is less observed with lipophilic ARIs containing hydroxyl moieties than with rigid ARIs which interact with the enzyme only through van der Waals' interactions. A possible explanation for this observation assumes destabilization during purification with some unfolding of lipophilic (van der Waals' interactive) regions at the inhibitor site while the adjacent hydrogen bonding regions are less affected. Nucleotide binding has been observed to change with modification of ^{298}Cys so that a weakened interaction between the NADPH and enzyme occurs presumably through altered interaction with the 2'-monophosphoadenoside 5'-disphosphoribose of NADPH and enzyme.[40] This resulted in reduced inhibitory activity for inhibitors such as sorbinil while quercetin or tolrestat were less affected. The present model in which the adenine ring forms the primary lipophilic binding region is also in agreement with these observations. Structurally rigid compounds such sorbinil are primarily bound and aligned to the adenine ring by van der Waals' interactions which in turn positions the 2'-carbonyl group for nucleophilic interaction with residues on the enzyme. In contrast compounds such as quercetin are anchored onto the site by multiple hydrogen bonding and interaction with the secondary lipophilic (van der Waals' interactive) site in addition to van der Waals' interactions with the adenine. As a result, changes in the positioning of the adenine ring would be expected to affect the proper alignment of sorbinil for interaction with the enzyme to a greater extent than it would with quercetin.

Limited docking studies with sorbinil and its N-methyl analog have also been conducted on the substrate binding region identified by co-crystallization with zopolrestat. This substrate site, which is comprised of the nicotinamide portion of NADPH, ^{48}Tyr, ^{110}His and ^{298}Cys, is much larger and less sterically hindered than the presently proposed AR·NADPH·I site, so that compounds bind with larger interaction energies. Based on diagrams of the published AR-zopolrestat complex,[8] the interaction energy of zopolrestat was computed to be –41.8 kcal mol^{-1}. Substituting sorbinil in place of zopolrestat so that the negative charge of the hydantoin ring corresponds with the carboxyl group of zopolrestat resulted in a ΔE value of –38.3 kcal mol^{-1}. Subsequently turning the sorbinil molecule so that the negative charge of the hydantoin ring faced the opposite direction resulted in a similar value of –42.9 kcal mol^{-1}. Substituting sorbinil with its inactive and neutrally charged N-methyl analog resulted in an energy value of –29.4 kcal mol^{-1} for the initial conformation and –37.4 kcal mol^{-1} for the corresponding opposite conformation, a decrease of –8.9 and –5.5 kcal mol^{-1}, respectively. These results do not support the observed stereospecific inhibition of aldose reductase by sorbinil and published structure activity results.

While the observed binding of zopolrestat to the substrate site cannot be disputed, specific binding of structurally diverse aldose reductase inhibitors to this site is not supported by observed experimental kinetic, SAR, affinity and photoaffinity studies and quantum chemical calculation. The presently proposed alternate site contains a number of pharmacophoric elements previously proposed for the inhibitor site and docking studies with a variety of structurally diverse inhibitors are consistent with a number of observed experimental studies.

Acknowledgement

The authors wish to thank Dr Lewis Pannell of NIADDK for the mass spectroscopy.

References

1. The Diabetes Control and Complications Trial Research Group *New England J. Med.* **1993**, *29*, 977.

2. Kador, P. F. *Medicinal Research Reviews* **1988**, *8*, 325.

3. Kador, P. F.; Akagi, Y.; Takahashi, Y.; Ikebe, H.; Wyman M.; Kinoshita J. H. *Arch. Ophthalmol.* **1990**, *108*, 1295.

4. Kador, P. F.; Takahashi, Y.; Sato, S.; Wyman, M *Preventive Medicine* **1994**, *23*, 717.

5. Masson, E. A.; Boulton, A. J. M. *Drugs* **1990**, *39*, 190.

6. Wilson, D. K.; Bohren, K. M.; Gabbay, K. H.; Quiocho, F. A. *Science* **1992**, *257*, 81.

7. Harrison, D. H.; Bohren, K. M.; Ringe, D.; Petsko, G. A.; Gabbay, K. H. *Biochemistry* **1994**, *33*, 2011.

8. Wilson, D. K.; Tarle, I.; Petrash, J. M.; Quiocho, F. A. *Proc. Natl. Acad. Sci. U.S.A.* **1993**, *90*, 9847.

9. Sarges, R. *Adv. Drug Res.* **1989**, *18*, 139.

10. Humber, L. G. *Prog. Med. Chem.* **1987**, *24*, 299.

11. Smar, M. W.; Ares, J. J.; Nakayama, T.; Itabe, H.; Kador, P. F.; Miller, D. D. *J. Med. Chem.* **1992**, *35*, 1117.

12. Sestanj, K.; Simard-Duuesne, N.; Dvornik D. M. U.S. Patent 3,821,383, 1974.

13. Old, S. E.; Sato, S.; Kador, P. F.; Carper, D. A. *Proc. Natl. Acad. Sci. U.S.A.* **1990**, *87*, 4942.

14. Sato, S. *Invest. Ophthalmol. Vis. Sci.* **1993**, *34*, 3172.

15. Bradford, M. M. *Anal. Biochem.* **1976**, *72*, 248.

16. Laemmli, U. K. *Nature* **1970**, 15, 680.

17. Brooks, B. R.; Bruccoleri, R. E.; Olafson, B. D.; States, D. J.; Swaminathan, S.; Karplus, M. J.; *Comp. Chem.* **1983**, *4*, 187.

18. Parameter File for CHARMm22, Molecular Simulations Inc., Waltham, MA, 1992.

19. Steinbach, P. J.; Brooks, B. R. *J. Comp. Chem.* **1994**, *15*, 667.

20. Sato, S.; Old, S.; Carper, D.; Kador, P. F. *Adv. Exp. Med. Biol.* **1995**, *372*, 259.

21. Bohren, K. M.; Bullock, B.; Wermuth, B.; Gabbay, K. H. *J. Biol. Chem.* **1994**, *265*, 9547.

22. Kador, P. F.; Sharpless, N. E. *Mol. Pharmacol.* **1983**, *24*, 521.

23. Lee, Y. S.; Pearlstein, R.; Kador, P. F. *J. Med. Chem.* **1994**, *37*, 787.

24. Kador, P. F.; Sharpless, N. E.; Kinoshita, J. H. *J. Med. Chem.* **1985**, *28*, 841.

25. Kador, P. F.; Sharpless, N. E. *Biophys. Chem.* **1978**, *8*, 81.

26. Ward, W. H.; Cook, P. N.; Mirrlees, D. J.; Brittain, D. R.; Preston, J.; Carey, F.; Tuffin, D. P.; Howe, R. *Biochem. Pharmacol.* **1991**, *42*, 2115.

27. Ehrig, T.; Bohren, K. M.; Prendergast, F. G.; Gabbay, K. H. *Biochemistry* **1994**, *33*, 7157.

28. Ares, J. J.; Kador, P. F.; Miller, D. D. *J. Med. Chem.* **1986**, *29*, 2384.

29. Kador, P. F.; Gurley, R. C.; Ares, J. J.; Miller, D. D. *Prog. Clin. Biol. Res.* **1987**, *232*, 353.

30. Kador, P. F.; Nakayama, T.; Sato, S.; Smar, M.; Miller, D. D. *Prog. Clin. Biol. Res.* **1989**, *232*, 237.

31. Kador, P. F.; Goosey, J. D.; Sharpless, N. E.; Kolish, J.; Miller, D. D. *Eur. J. Med. Chem.* **1981**, *16*, 293.

32. O'Brien, M. M.; Schofield, P. J.; Edwards, M. R. *J. Neurochem.* **1982**, *39*, 810.

33. Bhatnagar, A.; Lui, S.; Das, B.; Ansari, N. H.; Srivastava, S. K. *Biochem. Pharmacol.* **1990**, *39*, 1115.

34. Grimshaw, C. E.; Shabaz, M.; Jahangiri, G.; Putney, C. G.; McKercher, S. R.; Mathur, E. J. *Biochemistry* **1989**, *28*, 5343.

35. Grimshaw, C. E. *Adv. Exp. Med. Biol.* **1990**, *284*, 217.

36. Griffin, B. W.; McNatt, L. G. *Arch. Biochem. Biophys.* **1986** *246*, 75.

37. Griffin, B. W.; McNatt, L. G.; York, Jr B. M. *Prog. Clin Biol Res.* **1987**, *232*, 325.

38. Larson, E. R.; Lipinski, C. A.; Sarges, R. *Medical Research Rev.* **1988**, *8*, 159.

39. Kador, P. F.; Sharpless, N. E.; Goosey, J. D. *Prog. Clin Biol. Res.* **1982**, *114*, 243.

40. Bhatnagar, A.; Liu, S.; Uneo, N.; Chakrabarti, B.; Srivastava, S. K *Biochim. et Biophys. Acta—Protein Structure and Mol. Enzymol.* **1994**, *1205*, 207.

41. Kador, P. F.; Kinoshita, J. H.; Sharpless, N. E. *Metabolism (Suppl 1)* **1986**, *35*, 109.

(*Received in U.S.A.* 2 *February* 1995; *accepted* 2 *June* 1995)